

**Supplementary Information for 'Generation and evolution of  
spin-, valley- and layer-polarized excited carriers in  
inversion-symmetric WSe<sub>2</sub>'**

R. Bertoni,<sup>1</sup> C. W. Nicholson,<sup>1</sup> L. Waldecker,<sup>1</sup> H. Hübener,<sup>2</sup> C.  
Monney,<sup>3</sup> U. De Giovannini,<sup>2</sup> M. Puppini,<sup>1</sup> M. Hoesch,<sup>4</sup> E. Springate,<sup>5</sup>  
R. T. Chapman,<sup>5</sup> C. Cacho,<sup>5</sup> M. Wolf,<sup>1</sup> A. Rubio,<sup>2,6</sup> and R. Ernstorfer<sup>1,\*</sup>

<sup>1</sup>*Fritz-Haber-Institut der Max-Planck-Gesellschaft,  
Faradayweg 4-6, 14195 Berlin, Germany*

<sup>2</sup>*Nano-Bio Spectroscopy Group and ETSF, Universidad del Pas Vasco,  
CFM CSIC-UPV/EHU, 20018 San Sebastian, Spain*

<sup>3</sup>*University of Zurich, Department of Physics,  
Winterthurerstrasse 190, 8057 Zurich, Switzerland*

<sup>4</sup>*Diamond Light Source, Harwell Campus,  
Didcot OX11 0DE, United Kingdom*

<sup>5</sup>*Central Laser Facility, STFC Rutherford Appleton Laboratory,  
Harwell Campus, Didcot OX11 0QX, United Kingdom*

<sup>6</sup>*Max Planck Institute for the Structure and Dynamics  
of Matter and Center for Free-Electron Laser Science,  
Notkestrae 85, 22761 Hamburg, Germany*

## TR-ARPES

Time- and angle-resolved photoemission (trARPES) experiments were performed at the Materials Science end-station at Artemis (Central Laser Facility, UK), employing femto second pump pulses in the visible and probe pulses in the EUV spectral regions at a repetition rate of 1 kHz. An optical parametric amplifier converts the pump-pulses to a central wavelength of 1520 nm. These pulses are then frequency doubled in a BBO crystal to obtain pump pulses of 760 nm central frequency (1.63 eV), slightly above the direct bandgap of WSe<sub>2</sub>, located at the K-points. A motorized quarter-wave plate is used to change the polarization of the pump pulses. EUV photons are obtained by high harmonic generation of the fundamental laser pulses in a pulsed argon gas jet. A time-preserving monochromator was used to reduce the obtained spectral width to the 15th harmonic (23 eV photon energy). The energy of the probe photons allows simultaneous measurement of the electronic dynamics at the K (K') and  $\Sigma$  points of the Brillouin zone and ensures maximum sensitivity of the experiment to electrons emitted from the topmost layer. Measurements at the inequivalent K and K' points were performed consecutively after rotating the samples along the K- $\Gamma$ -K' direction. The resulting angle of incidence of the pump and probe pulses on the sample were 15° for measurements at K' and 75° for measurements at K, respectively. The experiments were performed in ultra-high vacuum (UHV) at room temperature and 80 K (green triangles in Fig. 2b). Single crystals of WSe<sub>2</sub> were obtained from HQ Graphene (Netherlands) and cleaved in UHV prior to measurements. As the cleaving process leads to areas of different surface termination, the sample surface was scanned for maximum dichroic signal prior to the dichroism measurements.

## DFT CALCULATIONS

Band structure calculations of Fig. 1b, 1c and 3b were performed using the ABINIT package [1] within the local spin density approximation [2] and with optimized structural parameters for each geometry. We compare the electronic structure of a bilayer and a six-layer slab and find that the projected electronic structures of the topmost layers for both systems agree well, in particular with respect to the positions of the K and  $\Sigma$  valleys of the conduction band (CB). For the surface projection, the Kohn-Sham spinor is projected onto

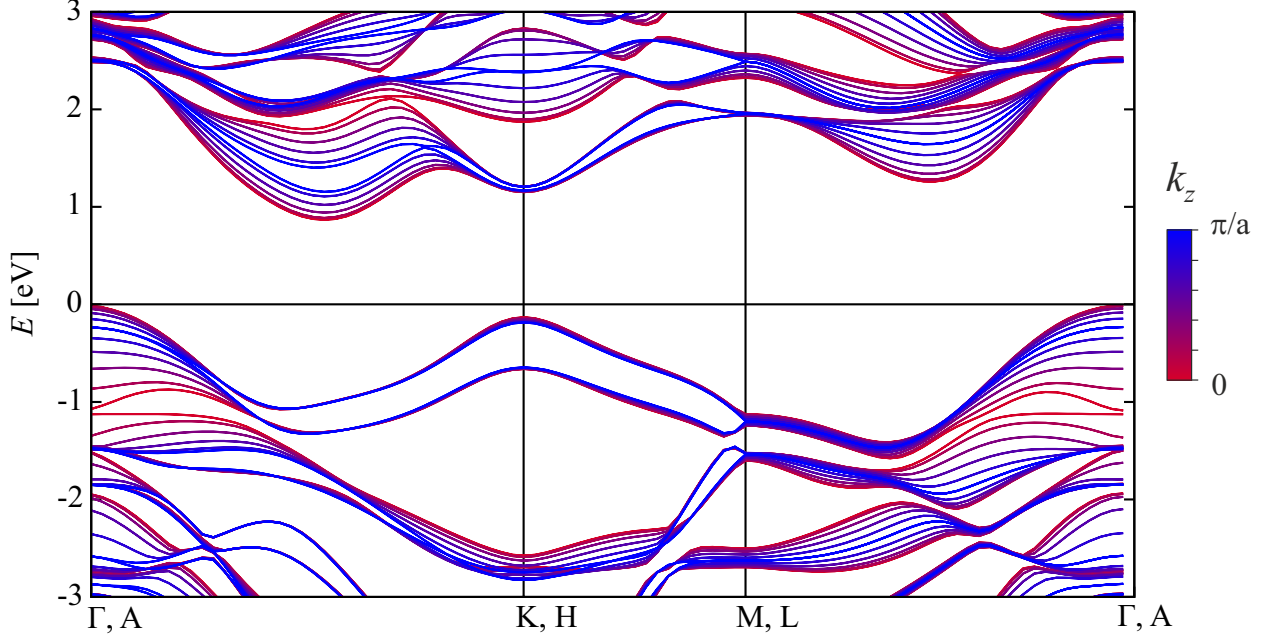


FIG. SM1. Dispersion of valence and conduction band states of bulk WSe<sub>2</sub> in six equidistant planes parallel to the  $\Gamma$ -K-M plane with  $k_z$  ranging from 0 to  $\frac{\pi}{a}$ .

the atoms of the top-most layer. The spin polarization is computed by projecting the Kohn-Sham spinor onto the  $S_z$  spin operator. The CB states are shifted in energy by 250 meV to match the experimental data. The evolution of the electronic structure under pump conditions, Fig. 2c, is computed by propagating the Kohn-Sham equations within TDDFT as provided by the octopus package [3]. The frequency of the pump field was tuned to the gap of the Kohn-Sham states at K. The excited state population is obtained by comparing the time-evolved valence states to the unoccupied states of the ground state. Over time, a growing overlap of a valence state with an unoccupied ground state indicates that the state is assuming the character of an excited state and thus its square modulus is interpreted as the transfer of electronic population to the excited state. All calculations were performed using the HGH pseudopotentials [4].

The dispersion of the bands in six equidistant planes parallel to the  $\Gamma$ -K-M plane with  $k_z$  ranging from 0 to  $\frac{\pi}{a}$  are shown in Fig. SM1. It is clear from these plots that the  $k_z$  dispersion of the states in the  $\Sigma$  valleys is significantly larger than of the states in K valleys points, confirming the assignment of 3D and 2D character of the states in the respective valleys.

## SCATTERING MODEL

The scattering of electrons was simulated by numerically solving a set of rate equations for the excited state populations  $P_i$ , with  $i = K, K', \Sigma$ . In the simulations, electronic population is created in the excited state at K, assuming a spin-selective excitation of contrast  $c=0.95$  for circularly polarized and  $c = 0.5$  for linearly polarized light. The excitation is taken to be proportional to the intensity of the laser pulse  $L(t)$ , the shape of which is modeled as a Gaussian function of FWHM 100 fs, close to the experimental conditions. Scattering is assumed to be mono-exponential with rates given as the inverse of the time constants  $b\tau_i$ . For comparison to the measured intensities  $I_i$ , weighting factors  $M_i$  are fitted as  $I_i = M_i \cdot P_i$  to account for differences of the photoemission matrix elements. Scattering is assumed to be symmetric between K and K', but asymmetric between K/K' and  $\Sigma$ , due to the energetic difference between the two valleys of around 250 meV, which is larger than the maximum phonon energy of around 35 meV [5] and is modelled by the factor  $\alpha$ . The set of equations is

$$\frac{\partial P_K}{\partial t} = -\frac{P_K - \alpha \cdot P_\Sigma}{\tau_{K\Sigma}} - \frac{P_K - P_{K'}}{\tau_{KK'}} + c \cdot L(t) \quad (1a)$$

$$\frac{\partial P_{K'}}{\partial t} = -\frac{P_{K'} - \alpha \cdot P_\Sigma}{\tau_{K\Sigma}} + \frac{P_K - P_{K'}}{\tau_{KK'}} + (1 - c) \cdot L(t) \quad (1b)$$

$$\frac{\partial P_\Sigma}{\partial t} = +\frac{P_K - \alpha \cdot P_\Sigma}{\tau_{K\Sigma}} + \frac{P_{K'} - \alpha \cdot P_\Sigma}{\tau_{K'\Sigma}} - \frac{P_\Sigma}{\tau_{\Sigma d}}. \quad (1c)$$

Because of the three-dimensional character of states at the  $\Sigma$  valleys,  $\Sigma$  and  $\Sigma'$  are indistinguishable, such that we take  $\tau_{K\Sigma} = \tau_{K\Sigma'} = \tau_{K'\Sigma}$ . As electrons in the  $\Sigma$  valleys can scatter away from the surface into the bulk, they are not observed by the experiment, which is accounted for by scattering to unobservable states with time constant  $\tau_{\Sigma d}$ . The four independent parameters  $\tau_{K\Sigma}$ ,  $\tau_{KK'}$ ,  $\tau_{\Sigma d}$  and  $\alpha$  of the equations are optimized by a non-linear solver to best reproduce the set of six measured time-traces. Values of  $\tau_i$  given in the main text and  $\alpha = 0.06 \pm 0.03$  are averages from fitting several datasets, and the given errors are the standard deviation of these values.

---

\* ernstorfer@fhi-berlin.mpg.de

- [1] X. Gonze, B. Amadon, P.-M. Anglade, J.-M. Beuken, F. Bottin, P. Boulanger, F. Bruneval, D. Caliste, R. Caracas, M. Côté, T. Deutsch, L. Genovese, P. Ghosez, M. Giantomassi, S. Goedecker, D. R. Hamann, P. Hermet, F. Jollet, G. Jomard, S. Leroux, M. Mancini, S. Mazevet, M. J. T. Oliveira, G. Onida, Y. Pouillon, T. Rangel, G.-M. Rignanese, D. Sangalli, R. Shaltaf, M. Torrent, M. Verstraete, G. Zerah, and J. Zwanziger, *Computer Physics Communications* **180**, 2582 (2009).
- [2] J. P. Perdew and A. Zunger, *Physical Review B* **23**, 5048 (1981).
- [3] X. Andrade, D. Strubbe, U. De Giovannini, A. H. Larsen, M. J. T. Oliveira, J. Alberdi-Rodriguez, A. Varas, I. Theophilou, N. Helbig, M. J. Verstraete, L. Stella, F. Nogueira, A. Aspuru-Guzik, A. Castro, M. A. L. Marques, and A. Rubio, *Phys. Chem. Chem. Phys.* **17**, 31371 (2015).
- [4] C. Hartwigsen, S. Goedecker, and J. Hutter, *Physical Review B* **58**, 3641 (1998).
- [5] H. Sahin, S. Tongay, S. Horzum, W. Fan, J. Zhou, J. Li, J. Wu, and F. M. Peeters, *Physical Review B* **87**, 165409 (2013).